Vietnam Journal of Science and Technology ***64***(2) (2026) 317–327
DOI: https://doi.org/10.15625/2525-2518/20757

Preparation and characterization of biomaterials based on polycaprolactone and chrysophanol

Nguyen Thuy Chinh[1,2], Trinh Hoang Nghia[3], Do Thi My[4], Ly Thi Ngoc Lien[1], Thai Hoang[1,2,*]

[1]*Institute for Materials Science, Vietnam Academy of Science and Technology, 18 Hoang Quoc Viet, Nghia Do ward, Ha Noi, 100000, Viet Nam*
[2]*Graduate University of Science and Technology, Vietnam Academy of Science and Technology, 18 Hoang Quoc Viet, Nghia Do ward, Ha Noi, 100000, Viet Nam*
[3]*Université du Québec à Trois - Rivières, 3351 Boulevard des Forges, Trois-Rivières, Québec, Canada*
[4]*Hanoi University of Industry, 298 Cau Dien, Tay Tuu ward, Ha Noi, 100000, Viet Nam*

[*]Email: *hoangth@itt.vast.vn*

Received: 9 May 2024; Accepted for publication: 7 June 2024

Abstract. Polymeric biomaterials based on biodegradable, non-toxic polymers are being studied for applications in pharmaceutical and medical fields. With their advantages, many products have been developed and tested over the past decades. Chrysophanol (CSP), a natural anthraquinone isolated from fungi, rhubarb, senna, etc., exhibits good properties such as hemostasis, antibacterial ability, anti-inflammatory, anti-cancer, and improving local blood deficiency conditions, etc. Despite its numerous beneficial effects, the poor water solubility of CSP limits its absorption in the body. Polycaprolactone (PCL), a biocompatible and biodegradable polyester, has been extensively researched for polymeric biomaterials carrying drugs to achieve controlled drug release, improve water solubility, and enhance drug bioavailability. This work presents the preparation and characterization of a novel biomaterials based on the PCL and CSP at different PCL/CSP ratios prepared by the solution method. The methods, including infrared (IR) spectroscopy, scanning electron microscopy (SEM), dynamic light scattering (DLS), X-ray diffraction (XRD), differential scanning calorimetry (DSC) and ultra violet visible (UV-Vis) spectroscopy, have been used to assess the characteristics of PCL/CSP biomaterials. The obtained results indicate that CSP was loaded by PCL and they can interact to each other through physical interactions. The presence of PCL in the biomaterials contributes significantly to enhancing the solubility of CSP in aqueous environment. As a result, the CSP content released from PCL/CSP biomaterials was improved remarkably in pH 2.0 and pH 7.4 buffer solutions. Additionally, the release kinetic of CSP from the biomaterials has been calculated to find a suitable mechanism for drug release in the simulated body fluids.

Keywords: biomaterials, polycaprolactone, chrysophanol, drug release, characterization.

Classification numbers: 2.3.1, 2.7.1.

1. INTRODUCTION

Plastic waste from polymers such as polyethylene and polypropylene is considered a global pollution agent. In recent years, numerous studies have been conducted to identify environmentally friendly bio-based materials. Polycaprolactone (PCL), a semi-crystalline polymer - is one such biodegradable material that is environmentally friendly and widely utilized in the medical field due to its biological compatibility and ability to degrade by hydrolyzing ester bonds under physiological conditions [1-3]. The PCL is a hydrophobic synthetic polymer with high flexibility and biocompatibility, soluble in various solvents at room temperature but insoluble in alcohols, petroleum, etc. As a result, the PCL is applied in controlled drug delivery systems [4, 5], tissue engineering [6, 7], wound healing techniques [8, 9], etc. The PCL has been approved by the US Food and Drug Administration (FDA) for internal medical applications due to its low immunogenicity [10, 11].

Several drug delivery systems including PCL in the forms of microspheres, nanocapsules, nano-spheres, and nano-fibers have been developed for controlled release of drugs or proteins [4, 5, 11-13]. The biodegradable nature of PCL fibers has paved the way for research on drug release control. Yan *et al.* successfully fabricated pH-sensitive core-shell nanofibers of PCL/polyvinyl alcohol (PCL/PVA), where the PCL is core and PVA is shell. These nano fibers can be efficiently degraded under acidic or neutral conditions. Moreover, the PCL/PVA fibers can serve as drug carriers for the anti-cancer drug paclitaxel (PTX) [12]. Williamson *et al.* combined a hydrophilic macromolecule (ovalbumin) and a hydrophilic drug (progesterone) within PCL fibers using the gravitational spinning method for particle dispersion [13]. Chang *et al.* incorporated gentamicin sulfate (GS) into PCL fibers through gravitational spinning method to create biomaterials capable of locally controlling antibiotic distribution. The drug release kinetics can be adjusted by varying the amount of GS within the fibers and the fabrication conditions [14]. Puppi *et al.* optimized wet spinning conditions to obtain 3D scaffolds of PCL loaded with antibiotics enrofloxacin (EF) and levofloxacin (LF). Most antibacterial agents added to the polymer solution had blood-clotting ability, and the drug loading efficiency ranged from 18 % to 27 %, depending on the antibiotic type and concentration. The polymer systems carrying EF and LF exhibited rapid drug release initially, followed by sustained release for up to 5 weeks [15]. Luong and Liu have been applied the electrospinning method for preparation of PCL nanofibers for loading drugs such as heparin, ampicillin [16, 17].

Chrysophanol (CSP), also known as 1,8-dihydroxy-3-methyl-anthraquinone and chrysophanic acid with the chemical formula $C_{15}H_{10}O_4$, is a natural anthraquinone isolated from fungi, medicinal plants belonging to various plant families such as *Rhamnaceae* (buckthorn, cascara), *Polygonaceae* (rhubarb), *Caesalpiniaceae* (senna), etc. [18-20]. The CSP exists as a crystalline solid, typically appearing as a yellow-orange to reddish-brown powder, poorly soluble in water, slightly soluble in cold ethanol, readily soluble in hot ethanol, benzene, chloroform, ether, acetic acid, and acetone, among others [21]. With pharmacological effects such as anti-cancer, anti-inflammatory, antioxidant properties, the CSP has garnered attention from many scientists for research purposes [20, 21]. Studies have shown its potential in alleviating nerve cell damage induced by lead exposure in neonatal mice, inhibiting the viability of HepG2 cells over time, and reducing inflammation markers in lung-injured mice treated with paraquat [22-24]. Its pharmacokinetics, including plasma protein binding and tissue distribution, have also been investigated, highlighting its preferential binding to human serum compared to mouse serum and bovine serum albumin [25]. Despite its valuable medicinal properties, the limited water solubility of CSP poses a challenge in formulation and delivery methods.

The combination of PCL and CSP in the biomaterials is still limited in research. Therefore, the aim of this study is to prepare the biomaterials based on PCL and CSP by solution method and to characterize these biomaterials using infrared (IR) spectroscopy, scanning electron microscopy (SEM), dynamic light scattering (DLS), X-ray diffraction (XRD), differential scanning calorimetry (DSC) and ultra violet visible (UV-Vis) spectroscopy. Additionally, the drug release content and drug release kinetics of CSP from PCL/CSP biomaterials in simulated body fluids have been also assessed and discussed.

2. MATERIALS AND METHODS

2.1. Materials

Polycaprolactone (PCL, average M_w ~14,000, average M_n ~10,000 by GPC) and chrysophanol (CSP, ≥ 98 % by HPLC, melting point of 192-196ºC) were purchased from Sigma Aldrich. The solvents used were dichloromethane (DCM, 99 %, China) and ethanol (99.5 %, China).

2.2. Preparation of PCL/CSP biomaterial

0.1 g PCL was weighed and added to 25 mL of DCM before being stirred magnetically to obtain PCL solution. 0.001 g of CSP was weighed and dissolved in 10 mL of DCM. Next, the CSP solution was dropped slowly to the PCL solution in combining with magnetically stirring. The mixture was then homogenized by IKA T18 device for 30 minutes and following magnetically stirred for 2 hours. The mixture was poured into a petri dish and placed in room temperature for natural solvent evaporation to obtain PCL/CSP biomaterial in a powder form.

Table 1. Composition and abbreviation of PCL/CSP biomaterials.

No.	PCL/CSP ratio	PCL weight (g)	CSP weight (g)	Sample abbreviation
1	PCL/CSP = 100/1	0.1	0.001	PCL/CSP 1%
2	PCL/CSP = 100/2	0.1	0.002	PCL/CSP 2%
3	PCL/CSP = 100/3	0.1	0.003	PCL/CSP 3%
4	PCL/CSP = 100/5	0.1	0.005	PCL/CSP 5%
5	PCL/XG = 100/10	0.1	0.01	PCL/CSP 10%

2.3. Characterization

IR spectra of PCL/CSP biomaterial samples were recorded using a Nicolet iS10 spectrometer (USA) with conditions: wavenumbers ranged from 4000 to 400 cm^{-1}, scans of 16 times, resolution of 8 cm^{-1}. The morphology of PCL/CSP biomaterial samples was taken using a S4800 scanning electron microscopy (Hitachi, Japan). The size distribution of PCL/CSP biomaterial samples was determined by DLS method using a SZ-100Z2 device (Horiba, Japan). DSC204F1 device (Netzsch, Germany) has been used to record the differential scanning calorimetry (DSC) diagrams of PCL/CSP biomaterial samples. X-ray diffraction (XRD) analysis of PCL/CSP biomaterial samples was conducted using a D5000 X-ray diffractometer (Siemens, Germany) with conditions: 2 theta (θ) ranged from 10 to 80º, an X-ray CuKα incident beam with a wavelength of 0.154 nm. The UV - Vis spectroscopy (UV-Vis Libra S80, Biochrom, UK) was used to assess the CSP release content from PCL/CSP biomaterial samples.

2.4. Drug release study

The calibration equations of CSP in pH 2.0 and pH 7.4 buffer solution were set up dilution method and calculated based on absorbance values of CSP solutions obtained from UV-Vis analysis. The experiment for the drug release study of PCL/CSP biomaterial samples was carried out as follows: 0.015 g of PCL/CSP biomaterial samples and CSP (as a control sample) were weighed and put in a dialysis bag before being added to a 250 mL glass baker, following adding 150 mL of a buffer solution. The mixture was then stirred magnetically at 37 ºC for 7 hours with a speed of 400 rpm. After every hour of testing, 5 mL of mixture was withdrawn before being added with 5 mL of fresh buffer to the mixture to maintain the volume. The withdrawn solution was taken UV-Vis spectrum in the wavelength range of 200 – 400 nm. The CSP release content was calculated by this equation:

$$\%CSP = \frac{m_t}{m_o}.100 \quad (1)$$

where, m_t and m_o are the weight of CSP in the solution at t time and initial time, respectively.

After the suitable sample was found, the drug release process was carried out in both pH 2.0 (for 3 hours) and pH 7.4 solutions (following hours).

The drug release kinetics of CSP from the PCL/CSP biomaterial samples could be calculated based on some popular kinetic models, including zero-order kinetic, first-order kinetic, Higuchi model, Hixson-Crowell model, Korsmeyer – Peppas model as reported in several kinds of literature [15, 16].

3. RESULTS AND DISCUSSION

3.1. IR spectra

The IR spectrum of CSP is displayed in Figure 1. It can be seen the vibration of OH and CH bond in the benzene ring at wavenumber of 3056 cm^{-1}, the vibration of C=O at 1675 cm^{-1}, the vibration of C=C in the benzene ring at 1625 cm^{-1} [26, 27]. The bending vibration of C-H, O-H and stretching vibration of C-O, C-C were also observed in the wavenumbers ranging 1024 – 1567 cm^{-1}.

Figure 2 presents the IR spectra of PCL and PCL/CSP biomaterials. From the IR spectrum of PCL, there are sharp peaks that are characterized by vibrations of C-H, C=O, C-O, and C-C linkages in the structure of PCL. For instance, the stretching vibration of C-H linkages is located at 2940 and 2865 cm^{-1} while their bending vibration is assigned at 1469 and 1365 cm^{-1}. The peak at 1721 cm^{-1} is attributed to the stretching vibration of C=O linkages. The stretching vibrations of C-C, and C-O linkages were found in wavenumber ranging from 1044 to 1292 cm^{-1} [1, 9]. As can be observed from IR spectra of PCL/CSP biomaterials, the vibrations of both PCL and CSP appeared in these samples. This means that the biomaterials were composed of PCL and CSP. Moreover, when increasing CSP contents, the intensity of the peak at 1626 cm^{-1}, which characterized for C=C in the benzene ring of CSP, was increased. The benzene ring at 3054 cm^{-1} of CSP only observed on the IR spectrum of PCL/CSP10% sample may be due to the high content of CSP and the weak absorption of this peak. So, the content of CSP exhibits a slight effect on the intensity of vibrations characterized for functional groups of PCL/CSP biomaterials [27].

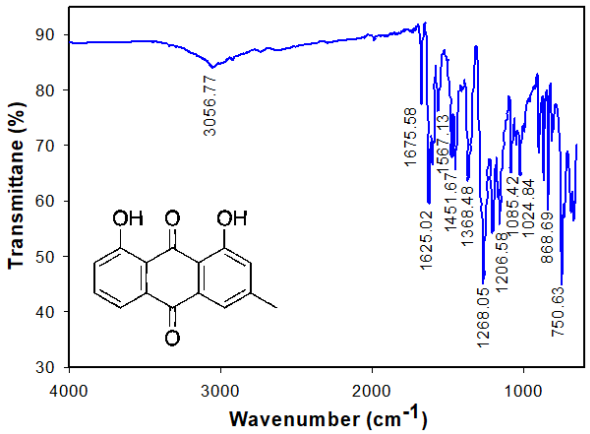

Figure 1. IR spectrum of CSP.

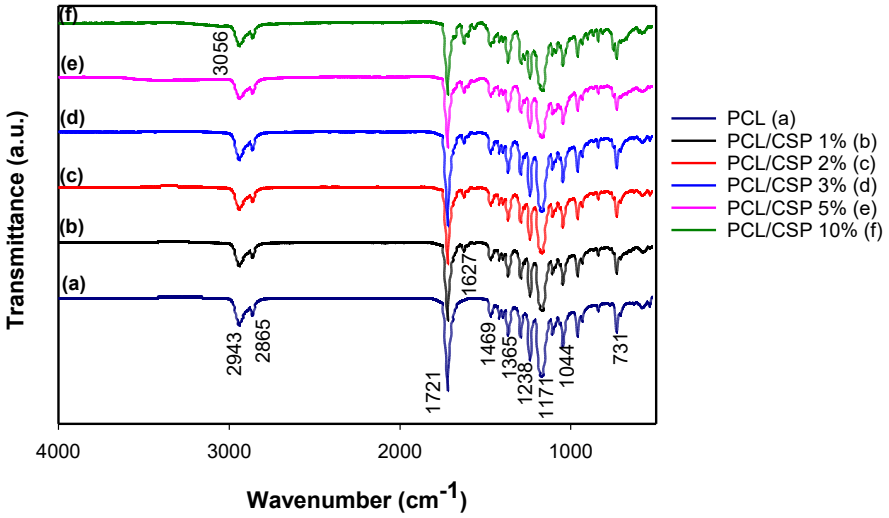

Figure 2. IR spectra of PCL and PCL/CSP biomaterials.

3.2. Morphology

The naked-eye and SEM images of PCL/CSP samples are shown in Figure 3. It can be observed that CSP content exhibited a significant effect on the morphology of PCL. The PCL is in white powder form with a smooth surface (Figure 3 A1, A3, A3). The PCL/CSP samples have a yellow color and are lighter than that of CSP. The PCL and PCL/CSP samples existed in block shape with a size of approximately 10-20 µm. When observing at a magnification of 50,000 times, the CSP was dispersed in a nano size of approximately 50-100 nm in the PCL matrix (Figure 3 B3-F3). The density and size of CSP increased as increasing CSP content in PCL. At high contents of CSP (5 and 10 wt.%), an agglomeration of CSP nanoparticles in the PCL matrix appeared clearly. Based on the analysis result of the SEM images, the CSP content ≤ 3 wt.% in PCL is suitable for PCL/CSP biomaterials having a regular structure [27].

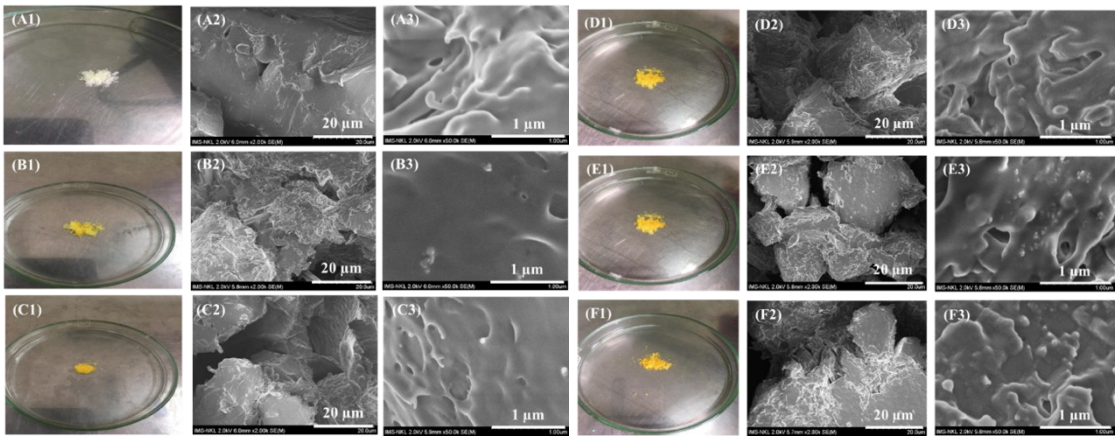

Figure 3. Naked-eye images and SEM images of PCL and PCL/CSP biomaterials. PCL (A1, A2, A3); PCL/CSP 1 % (B1, B2, B3); PCL/CSP 2 % (C1, C2, C3); PCL/CSP 3 % (D1, D2, D3); PCL/CSP 5 % (E1, E2, E3); PCL/CSP 10 % (F1, F2, F3).

3.3. Size distribution

The size distribution in ethanol solvent of PCL and PCL/CSP 3 % samples was indicated in Figure 4(a). It can be seen that CSP was distributed in ethanol by two peak sizes, the first peak ranged from 218 nm to 315 nm and the second peak ranged from 1207 nm to 1967 nm. The average particle size of CSP is 4278.3 ± 502.5 nm with a polydispersity index (PI) of 1.153 ± 0.188. Different from CSP, the PCL/CSP 3 % sample was distributed in ethanol by one peak size, from 655 nm to 1541 nm. The average particle size of the PCL/CSP 3 % sample is 1279.0 ± 120.5 nm with a PI of 0.465 ± 0.169. This result suggests that the PCL carrier helped to improve the distribution of CSP in ethanol solvent. The PCL/CSP 3 % sample exhibits a better distribution ability in ethanol, resulting in its smaller average particle size and PI value. This is also favorable for the solubility of PCL/CSP biomaterials in treatment.

3.4. DSC analysis

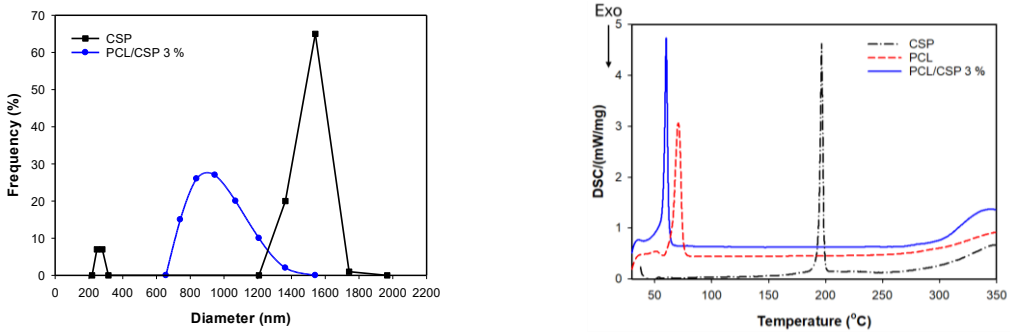

(a) (b)

Figure 4. Size distribution diagrams of CSP, and PCL/CSP 3 % in ethanol (a) and DSC diagrams of PCL, CSP, and PCL/CSP 3 % (B).

Figure 4(b) presents the DSC diagrams of CSP, PCL, and PCL/CSP 3 % sample. The CSP exhibits a sharp endothermic peak at 196.9°C (ΔH_f = 89.96 J/g), caused by the melting of CSP. A

similar outcome has been previously reported [27]. The PCL exhibits a small endothermic peak at around 51.3 ºC and a sharp and endothermic melting point at around 70.6 °C (ΔH_f = 102.3 J/g) [9]. The DSC analysis of the PCL/CSP 3 % sample showed that all excipients did not exhibit any thermal signals or individual melting peaks. This allowed for an exploration of potential interactions between the CSP and PCL in the PCL/CSP 3 % sample, which displayed a distinct endothermic peak at 60.1ºC (ΔH_f = 87/66 J/g) as well as the intensity of the endothermic peak of PCL/CSP 3 % much higher than that of the PCL. The physical interactions between drug and polymer through the hydrogen bonding of the -COO group in PCL with the hydroxyl group of CSP as presented in Figure 5(a) and mentioned in several previous reports [9, 27].

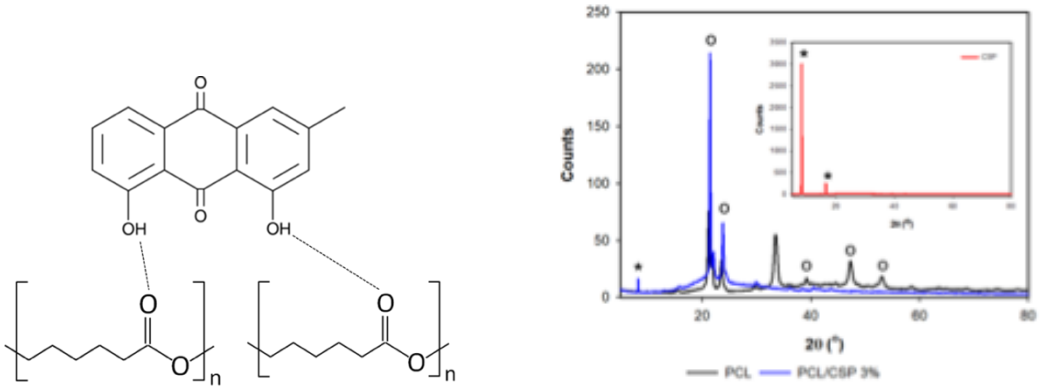

(a) (b)

Figure 5. Hypothesis interactions between PCL and CSP and XRD patterns of PCL, CSP, and PCL/CSP 3 %. (*) CSP crystallite, (o) PCL crystallite.

3.5. XRD analysis

Figure 5(b) exhibits the XRD patterns of PCL, CSP and PCL/CSP 3 % sample. The XRD analysis showed the crystalline structure of CSP and the partially crystalline structure of PCL. For instance, the CSP exhibits two diffraction peaks of crystallinity, at 2θ of 8.294° and 16.287°, corresponding to (100) and (200) plans [27]. The PCL distinguishes two main diffraction peaks of crystallinity, at 2θ of 21.443° and 24.342°, corresponding to (110) and (201) plans, respectively [9]. Other diffraction peaks of PCL were assigned at 2θ of 33.733°, 39.312°, 47.306°, and 52.230°. As compared to the XRD of the PCL, the XRD pattern of the PCL/CSP 3 % sample indicates that a new diffraction peak appeared at 8.294°, corresponding to the CSP crystalline, and some diffraction peaks of PCL at 2θ of 33.733°, 39.312°, 47.306° and 52.230° were absent. Additionally, the intensity of diffraction peaks of PCL crystalline was increased significantly. These findings are thus corroborating the interaction and inclusion of CSP in the PCL matrix. Moreover, the intensity of the diffraction peak of CSP crystalline is dramatically reduced, suggesting that CSP is no longer present in the crystalline form when loaded in PCL and exists in the amorphous state or the monomolecular dispersed state as reported previously [27-29].

3.6. Drug release content and drug release kinetics

The drug release content of CSP in simulated body fluids was calculated owing to the calibration equations of CSP in pH 2.0 buffer solution (y = 43.577x – 0.0049, R^2 of 0.9971) and pH 7.4 buffer solution (y = 39.178x -0.0005, R^2 of 0.9976), in which y represents optical density

or absorbance in UV-Vis spectrum and x represents the concentration of CSP in solution.

Figure 6(a) performs the CSP release content from investigated samples including CSP control and PCL/CSP biomaterials. The CSP exhibits poor solubility in pH 2.0 solution, with the CSP release content reaching 1.60 % after 7 hours of testing. When combining CSP with PCL, the solubility of CSP was increased remarkably and the CSP release process from PCL/CSP samples is continuous and quite stable. For example, after 7 hours of testing, the CSP release content from PCL/CSP 1%, PCL/CSP 2%, PCL/CSP 3%, PCL/CSP 5%, and PCL/CSP 10% reached 57.65, 77.49, 89.82, 66.18, and 63.62 %, respectively. The increase in the solubility of CSP was also achieved as a combination of CSP with a phospholipid [27]. The PCL also exhibits the role of an effective carrier for other drugs, such as curcumin [9], gentamicin sulfate [14], and ampicillin [17]. Thus, in this study, the PCL contributed importantly to the CSP release in the buffer solution. The increase in CSP drug release content also may be caused by the reduction of the crystalline degree of CSP in the biomaterial as indicated in the XRD analysis result. The initial content of CSP also influences the drug release content from PCL/CSP samples [30, 31]. This may be due to the difference in the distribution of CSP in the PCL matrix as mentioned in SEM analysis. The regular distribution of CSP in the polymer matrix helped to control the drug release better.

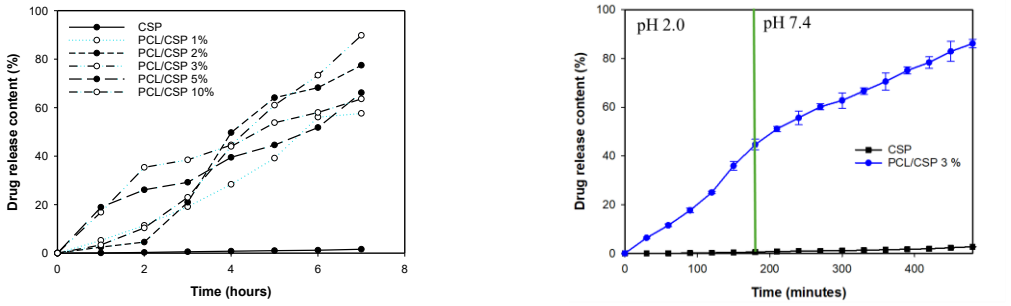

(a) (b)

Figure 6. Drug release content from PCL/CSP biomaterials in pH 2.0 buffer solution (a) and drug release content from PCL/CSP 3% in pH 2.0 and pH 7.4 buffer solutions (b).

The PCL/CSP 3 % exhibits the greatest drug release content, therefore, this sample would be chosen for the simulated drug release study in both pH 2.0 (corresponding to the gastric environment) and pH 7.4 (corresponding to the intestine environment) solutions. The results obtained are presented in Figure 6(b). It can be seen that CSP exhibits poor solubility in both pH 2.0 and pH 7.4 solutions while the PCL/CSP 3 % sample exhibits much better solubility. The drug release process is continuous in the pH 2.0 first and pH 7.4 following. In the pH 7.4 solution, the drug release from the PCL/CSP 3 % sample is quite linear, reflecting the linear dependence of drug concentration on time. This result also indicated that the drug can be released partially in the gastric environment and sustained release in the intestine environment.

The drug release kinetics of CSP from the PCL/CSP biomaterial samples could be calculated based on some popular kinetic models, including zero-order kinetic (ZO), first-order kinetic (FO), Higuchi model (HG), Hixson-Crowell model (HC), Korsmeyer – Peppas model (KP) as reported in several literatures [15, 16]. The regression coefficient (R^2) obtained by fitting these models is listed in Table 2. Based on R^2 values in Table 2, the CSP released from the CSP control sample was followed by the HC model in both pH 2.0 and pH 7.4 solutions while CSP released from the PCL/CSP 3% sample complied with the HC model in the pH 2.0 solution and the ZO kinetic in the pH 7.4 solution. This means that the release of CSP from the CSP control sample is the erosion

of CSP crystalline under the impact of ions in buffer solutions; the release of CSP from the PCL/CSP 3% sample occurred by the erosion from the surface's sample in the pH 2.0 solution and following the diffusion of the drug into the environment with a drug release concentration not changing over time and the concentration release rates remaining constantly [16, 30].

Table 2. The R^2 of kinetic models reflecting the release of CSP from the CSP control and PCL/CSP 3% sample in pH 2.0 and pH 7.4 buffer solutions.

Sample	R^2				
	ZO	FO	HG	HC	KP
pH 2.0 solution					
CSP	0.9448	0.9769	0.8797	0.9939	0.9779
PCL/CSP 3%	0.9827	0.9789	0.9378	0.9965	0.9795
pH 7.4 solution					
CSP	0.9421	0.9904	0.9859	0.9957	0.9892
PCL/CSP 3%	0.9985	0.9269	0.9788	0.9675	0.9350

4. CONCLUSIONS

The polycaprolactone (PCL)/chrysophanol (CSP) biomaterials with different contents of CSP were prepared by using the solution method. The IR, DSC, and XRD analysis results indicated that CSP can interact with PCL, leading to the reduction in the crystalline of CSP to an amorphous form. The CSP was dispersed regularly in the PCL matrix at the content below 3 wt.% and it tends to agglomerate to form clusters at higher CSP contents. When CSP is combined with PCL, the PCL/CSP biomaterials can distribute in ethanol much better than the CSP. The average particle size of the PCL/CSP 3 % sample reached 1279.0 ± 120.5 nm, much smaller than that of CSP, 4278.3 ± 502.5 nm. The CSP has poor solubility in the buffer solutions with the content of CSP release reaching only 0.56 ± 0.03 % in the pH 2.0 solution after 3 hours of testing and it reached 2.72 ± 0.14 % in the pH 7.4 solution for 5 following hours. For the PCL loading 3 wt.% CSP, it has a good solubility in the buffer solutions with the content of CSP release reaching 44.67 ± 2.23 % and 86.14 ± 1.72 % after 3 hours of testing in pH 2.0 solution and 5 following hours of testing in pH 7.4 solution. The release of CSP from the PCL/CSP 3 % sample complied with the Hixson-Crowell model in the pH 2.0 solution and the zero-order kinetic in the pH 7.4 solution. These findings indicate that PCL is a potential carrier for CSP, in particular, and for hydrophobic drugs, in general, to prepare biomaterials for biomedicine applications.

Acknowledgment. This research is funded by Vietnam National Foundation for Science and Technology Development (NAFOSTED) under grant number 104.02-2021.48.

CRediT authorship contribution statement. Nguyen Thuy Chinh: Investigation, Writing-original draft. Trinh Hoang Nghia, Do Thi My: Investigation. Ly Thi Ngoc Lien: Formal analysis. Thai Hoang: Conception, Writing-Reviewing and Editing, Supervision, Funding acquisition.

Declaration of competing interest. The authors declare that they have no known competing financial interests or personal relationships that could have appeared to influence the work reported in this paper.

REFERENCES

1. Lyu J. S., Lee J. S., Han J. - Development of a biodegradable polycaprolactone film incorporated with an antimicrobial agent via an extrusion process. Sci. Rep., **9**(1) (2019) 20236. https://doi.org/10.1038/s41598-019-56757-5.
2. Volokhova A. A., Kudryavtseva V. L., Spiridonova T. I., Kolesnik I., Goreninskii S. I., Sazonov R. V., Remnev G. E., Tverdokhlebov S. I. - Controlled drug release from electrospun PCL non-woven scaffolds via multi-layering and e-beam treatment. Mater. Today Commun., **26** (2021) 102134. https://doi.org/10.1016/j.mtcomm.2021.102134.
3. Radha S., Sudhir G. W., Roli P. - An overview on synthesis, properties and applications of polycaprolactone copolymers, blends & composites. Polym.-Plast. Technol. Mater., **62**(3) (2023) 327-358. https://doi.org/10.1080/25740881.2022.2113890.
4. Rai A., Senapati S., Saraf S. K., Maiti P. - Biodegradable poly(ε-caprolactone) as a controlled drug delivery vehicle of vancomycin for the treatment of MRSA infection. J. Mater. Chem. B, **4**(30) (2016) 5151-5160. https://doi.org/10.1039/c6tb01623e.
5. Pawar R., Pathan A., Nagaraj S., Kapare H., Giram P., Wavhale R. - Polycaprolactone and its derivatives for drug delivery. Polym. Adv. Technol., **34**(10) (2023) 3296-3316. https://doi.org/10.1002/pat.6140.
6. Samara R. P. O., Gabriely G. L., Marleane M. F. A., André S. A. F., Suziete B. S. G., Emerson S. N., Ricardo R. F. B., Francisco E. P. S., Lucielma S. S. P., Thiago D. S., Antônio M. M. F., Bartolomeu C. V., Anderson O. L., Gustavo O. M. G. - Controlled drug release from policaprolactone-piperine electrospun scaffold for bone tissue engineering. J. Drug Delivery Sci. Technol., **91** (2024) 105188. https://doi.org/10.1016/j.jddst.2023.105188.
7. Liu Y., Nelson T., Chakroff J., Cromeens B., Johnson J., Lannutti J., Besner G. E. - Comparison of polyglycolic acid, polycaprolactone, and collagen as scaffolds for the production of tissue engineered intestine. J. Biomed. Mater. Res. B Appl. Biomater., **107**(3) (2019) 750-760. https://doi.org/10.1002/jbm.b.34169.
8. Raina N., Pahwa R., Khosla J. K., Gupta P. N., Gupta M. - Polycaprolactone-based materials in wound healing applications. Polym. Bull., **79**(9) (2022) 7041-7063. https://doi.org/10.1007/s00289-021-03865-w.
9. Domínguez-Robles J., Cuartas-Gómez E., Dynes S., Utomo E., Anjani Q. K., Detamornrat U., Donnelly R. F., Moreno-Castellanos N., Larrañeta E. - Poly(caprolactone)/lignin-based 3D-printed dressings loaded with a novel combination of bioactive agents for wound-healing applications. Sustainable Mater. Technol., **35** (2023) e00581. https://doi.org/10.1016/j.susmat.2023.e00581.
10. Dhanasekaran N. P. D., Muthuvelu K. S., Arumugasamy S. K. - Recent Advancement in Biomedical Applications of Polycaprolactone and Polycaprolactone-Based Materials. In *Encyclopedia of Materials: Plastics and Polymers*, **4** (2022) 795-809.
11. Bhadran A., Shah T., Babanyinah G. K., Polara H., Taslimy S., Biewer M. C., Stefan M. C. - Recent Advances in Polycaprolactones for Anticancer Drug Delivery. Pharmaceutics, **15**(7) (2023) 1977. https://doi.org/10.3390/pharmaceutics15071977.
12. Yan E., Jiang J., Ren X., Gao J., Zhang X., Li S., Chen S., Li Y. - Polycaprolactone/polyvinyl alcohol core-shell nanofibers as a pH-responsive drug carrier for the potential application in chemotherapy against colon cancer. Mater. Lett., **291** (2021) 129516. https://doi.org/10.1016/j.matlet.2021.129516.
13. Williamson M. R., Chang H. I., Coombes A. G. A. - Gravity spun polycaprolactone fibres: controlling release of a hydrophilic macromolecule (ovalbumin) and a lipophilic drug (progesterone). Biomaterials, **25**(20) (2004) 5053-5060. https://doi.org/10.1016/j.biomaterials.2004.02.027.
14. Chang H. I., Lau Y. C., Yan C., Coombes A. G. A. - Controlled release of an antibiotic, gentamicin sulphate, from gravity spun polycaprolactone fibers. J. Biomed. Mater. Res., Part A, **84**(1) (2008) 230-237. https://doi.org/10.1002/jbm.a.31476.
15. Puppi D., Dinucci D., Bartoli C., Mota C., Migone C., Dini F., Barsotti G., Carlucci F., Chiellini F. - Development of 3D wetspun polymeric scaffolds loaded with antimicrobial agents for bone engineering. J. Bioact. Compat. Polym., **26**(5) (2011) 478-492. https://doi.org/10.1177/0883911511415918.

16. Luong V. E., Grondahl L., Chua K. N., Leong K. W., Nurcombe V., Cool S. M. - Controlled release of heparin from poly(ε-caprolactone) electrospun fibers. Biomaterials, **27**(9) (2006) 2042-2050. https://doi.org/10.1016/j.biomaterials.2005.10.028.
17. Liu H., Leonas K. K., Zhao Y. - Antimicrobial properties and release profile of ampicillin from electrospun poly(ε-caprolactone) nanofiber yarns. J. Eng. Fibers Fabr., **5**(4) (2010) 10-19. https://doi.org/10.1177/155892501000500402.
18. Genovese S., Tammaro F., Menghini L., Carlucci G., Epifano F., Locatelli M. - Comparison of three different extraction methods and HPLC determination of the anthraquinones aloe-emodine, emodine, rheine, chrysophanol and physcione in the bark of *Rhamnus alpinus* L. (Rhamnaceae). Phytochem. Anal., **21**(3) (2010) 261-267. https://doi.org/10.1002/pca.1195.
19. Jintao X., Yongli S., Liming Y., Quanwei Y., Chunyan L., Xingyi C., Yun J. - Near-infrared spectroscopy for rapid and simultaneous determination of five main active components in rhubarb of different geographical origins and processing. Spectrochim. Acta, Part A, **205** (2018) 419-427. https://doi.org/10.1016/j.saa.2018.07.055.
20. Xie L., Tang H., Song J., Long J., Zhang L., Li X. - Chrysophanol: a review of its pharmacology, toxicity and pharmacokinetics. J. Pharm. Pharmacol., **71**(10) (2019) 1475-1487. https://doi.org/10.1111/jphp.13143.
21. Prateeksha, Yusuf M. A., Singh B. N., Sudheer S., Kharwar R. N., Siddiqui S., Abdel-Azeem A. M., Fraceto L. F., Dashora K., Gupta V. K. - Chrysophanol: a natural anthraquinone with multifaceted biotherapeutic potential. Biomolecules, **9**(2) (2019) 68. https://doi.org/10.3390/biom9020068.
22. Zhang J., Yan C., Wang S., Hou Y., Xue G., Zhang L. - Chrysophanol attenuates lead exposure-induced injury to hippocampal neurons in neonatal mice. Neural Regener. Res., **9**(9) (2014) 924-930. https://doi.org/10.4103/1673-5374.133141.
23. Cui Y., Lu P., Song G., Liu Q., Zhu D., Liu X. - Involvement of PI3K/Akt, ERK and p38 signaling pathways in emodin-mediated extrinsic and intrinsic human hepatoblastoma cell apoptosis. Food Chem. Toxicol., **92** (2016) 26-37. https://doi.org/10.1016/j.fct.2016.03.013.
24. Li A., Liu Y., Zhai L., Wang L., Lin Z., Wang S. - Activating peroxisome proliferator-activated receptors (PPARs): a new sight for chrysophanol to treat paraquat-induced lung injury. Inflammation, **39**(2) (2016) 928-937. https://doi.org/10.1007/s10753-016-0326-2.
25. Chen Q., He H., Luo S., Xiong L., Li P. - A novel GC-MS method for determination of chrysophanol in rat plasma and tissues: Application to the pharmacokinetics, tissue distribution and plasma protein binding studies. J. Chromatogr. B, **973C** (2014) 76-83. https://doi.org/10.1016/j.jchromb.2014.10.011.
26. Jha R. N., Bajracharya G. B., Thakuri G. M. S., Gupta R. K. - Synthesis of antioxidative anthraquinones as potential anticancer agents. Bibechana, **18**(2) (2021) 143-153. https://doi.org/10.3126/bibechana.v18i2.31234.
27. Singh D., Rawat M. S. M., Semalty A., Semalty M. - Chrysophanol–phospholipid complex. J. Therm. Anal. Calorim., **111**(3) (2012) 2069-2077. https://doi.org/10.1007/s10973-012-2448-6.
28. Bruni G., Milanese C., Berbenni V., Sartor F., Villa M., Marini A. - Crystalline and amorphous phases of a new drug. J. Therm. Anal. Calorim., **102**(1) (2010) 297-303. https://doi.org/10.1007/s10973-009-0614-2.
29. Singh D., Rawat M. S. M., Semalty A., Semalty M. - Quercetin - phospholipid complex: an amorphous pharmaceutical system in herbal drug delivery. Curr. Drug Discovery Technol., **9**(1) (2012) 17-24. https://doi.org/10.2174/157016312799304507.
30. Nguyen T. C., Nguyen T. T. T., Nguyen V. G., Dinh T. M. T., To T. X. H., Nguyen Q. T., Chu Q. T., Pham M. Q., Pham Q. L., Thai H. - In vitro nifedipine release from poly(lactic acid)/chitosan nanoparticles loaded with nifedipine. J. Appl. Polym. Sci., **133**(16) (2016) 43330. https://doi.org/10.1002/app.43330.
31. Nguyen T. C., Thach T. L., Le D. G., Ngo P. T., Vu T. H., Thai H. - Effect of polycaprolactone on characteristics and morphology of alginate/chitosan/lovastatin composite films. Vietnam J. Sci. Technol., **56**(4B) (2018) 13-21. https://doi.org/10.15625/2525-2518/56/4A/12738.